Electronic Supporting Information

for

Multiple rotor modes and how to trigger them: Complex Cation Ordering in The Family of Relaxing Hybrid Formates

Paulina Peksa, Andrzej Nowok, Anna Gągor, Mirosław Mączka, Marek Drozd and Adam Sieradzki

1. Experimental details

Thermal Properties: Differential scanning calorimetry (DSC) runs were measured using Metler Toledo DSC-1 calorimeter with high resolution of 0.4 μW. Nitrogen was used as a purging gas, and the scanning rate was 5 K/min on a cooling and heating run. The sample weight was 27.95 mg. The excess heat capacity associated with the phase transition was evaluated by substraction of the baseline representing variation in the absence of the phase transition from the data.

The TGA study was performed in the temperature range 300-1130 K using a PerkinElmer TGA 4000. The sample weight was ca. 23.1 mg, and the heating speed rate was 10 K min^{-1}. Pure nitrogen gas an atmosphere was used.

Crystal structure investigations: The single-crystal x-ray diffraction was collected at 360, 300 and 120 K on Xcalibur, Atlas diffractometer using Mo *K*α radiation. Diffraction data were processed by *CrysAlis PRO* 1.171.38.43 (Rigaku Oxford Diffraction, 2015). The structures were solved and refined using SHELXL2018/3 (Sheldrick, 2018). H-atom parameters were constrained. The crystal data, data collection and refinement results are shown in details in Table S1 in ESI. Selected distances are given in Table S2, whereas hydrogen bond geometry in Table S3. **dptaMn** adopts two temperature induced polymorphs. The brief summary of their structures: Phase **I** (360 K)**,** trigonal *R*-3*c*, a=8.5557 (5) Å, c= 63.715 (4)Å; V=4039.1 (5)$Å^3$,

R(F2 > 2σ(F2)) =0.037, wR(F2)= 0.103, S=1.04; Phase **II (120 K),** monoclinic *I2/a***:** a=28.4792 (15) Å, b=8.6388 (4) Å, c=32.292 (3) Å, β=90.303(6) V=7944.5 (9) $Å^3$, R(F2 > 2σ(F2)) =0.064, wR(F2)= 0.129, S=1.17. The structures have been deposited in CCDC with deposition numbers 2100205 (120 K), 2100206 (360 K) and 2121379 (300 K).

Powder XRD (PXRD) patterns were collected on X'Pert PRO X-ray difractometer equipped with a PIXcel ultrafast line detector. The powders were measured in the reflection mode, using CuKα radiation. High temperature (HT) experiments were done in Anton Paar Oven Chamber.

Dielectric properties: The dielectric properties of single crystals were measured as a function of frequency and temperature by means of a broadband impedance Novocontrol Alpha analyzer. The samples were investigated isothermally at frequencies from 1 Hz to 1 MHz. The measurement were taken with an increment of 2 K over the temperature range from 130 to 360 K. Additionally, the temperature dependence of the dielectric permittivity was measured between 300K and 30 K and controlled using the helium gas cryostat for 1 MHz.

2. Supporting information for calorimetric studies

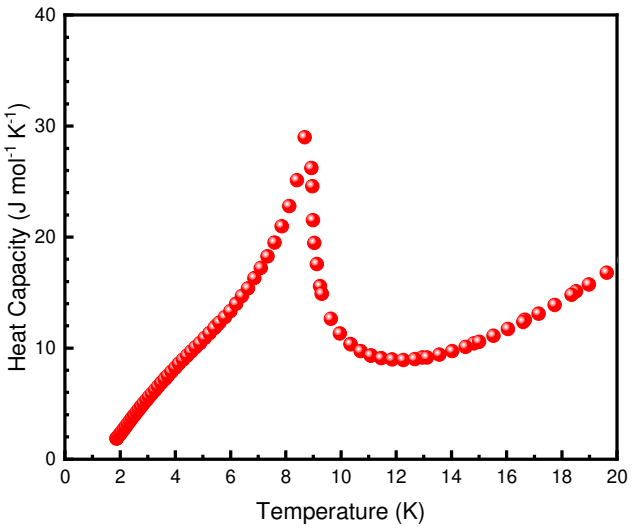

Fig.S1. *Results from adiabatic studies between 2K and 20K.*

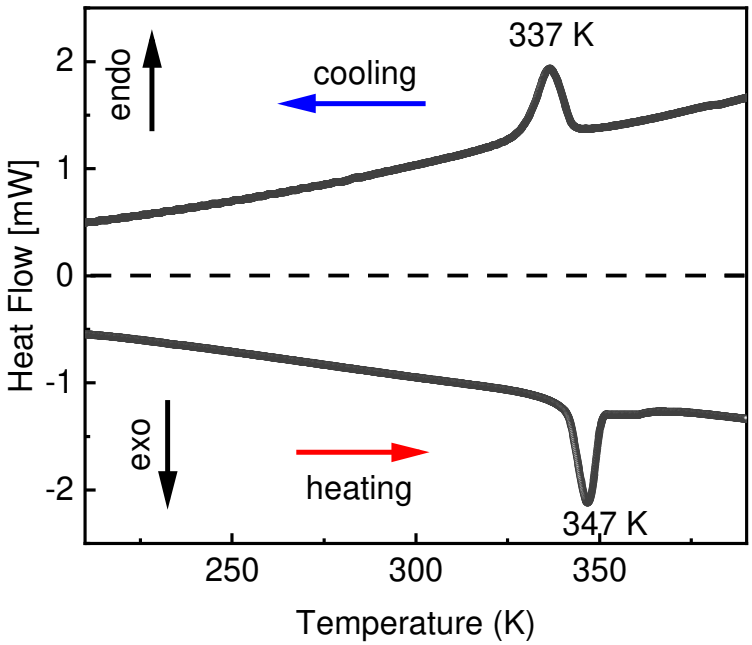

Fig.S2. *DSC data between 180K and 400K for cooling and heating scans.*

3. Supporting information for thermogravimetric analysis.

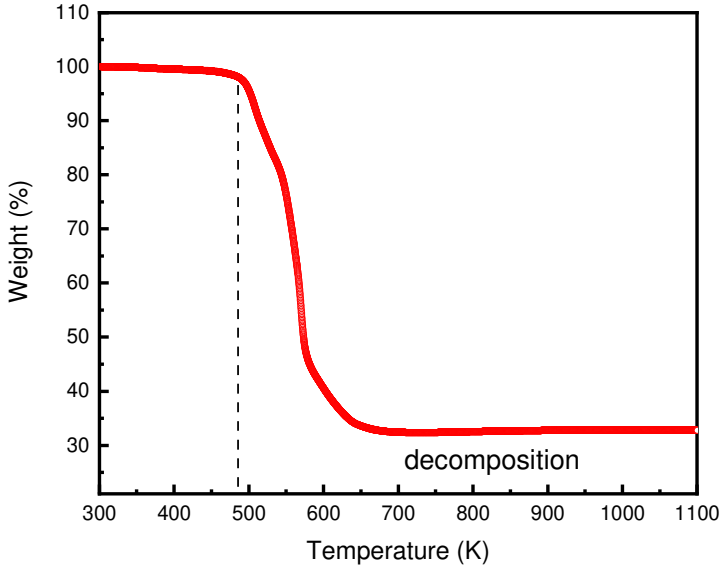

Fig.S3. *The results of the TGA analysis for* ***dptaMn****.*

4. Supporting information for X-ray diffraction studies

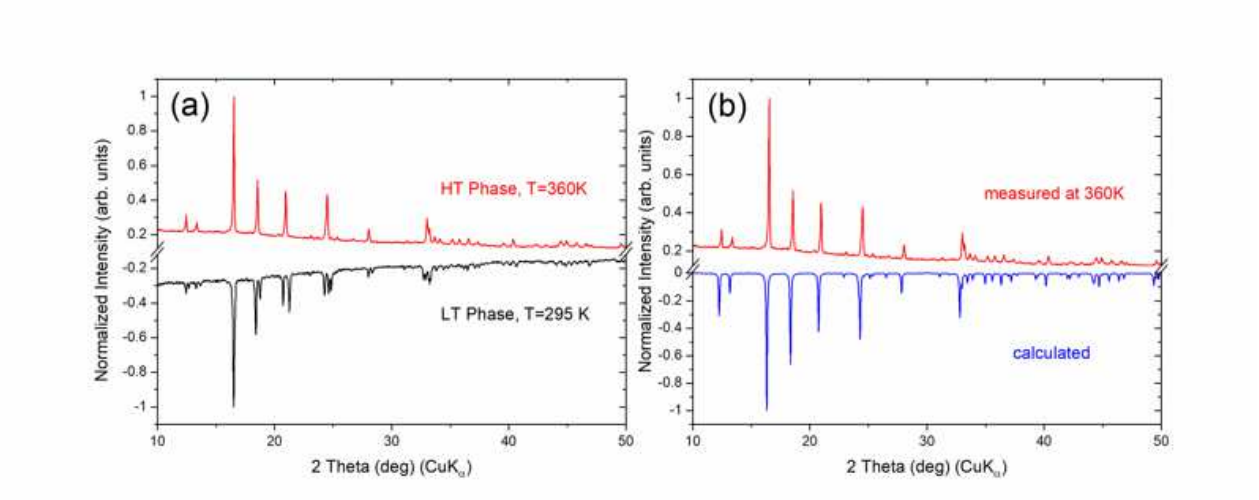

Fig.S4. *The results of the PXRD for (a) the high-temperature phase of* ***dptaMn*** *and low-temperature phase, (b) the high-temperature phase of* ***dptaMn*** *complied with calculated diffractogram. The calculated profile was obtained from the model from the single-crystal X-ray diffraction.*

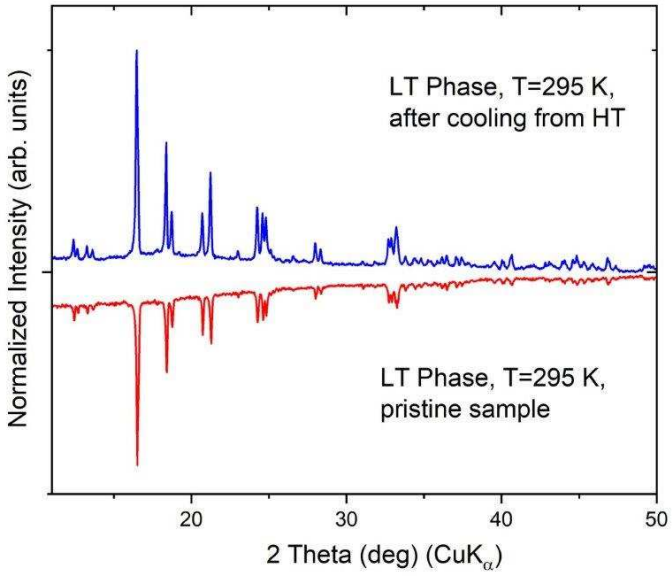

Fig.S5. *Powder diagram of pristine* ***dptaMn*** *crystals and after the phase transition from HT phase (from 360K).*

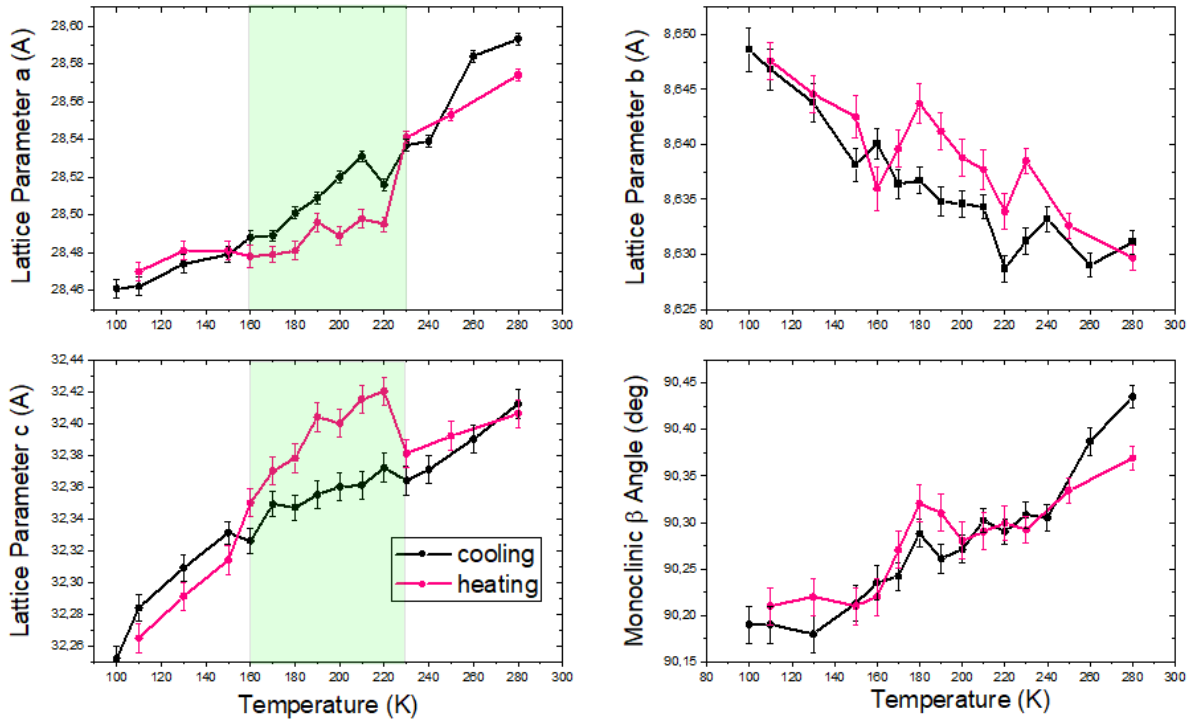

Fig.S6. *Thermal evolution of lattice parameters in the low-temperature phase II during cooling and heating.*

5. Supporting information for dielectric studies

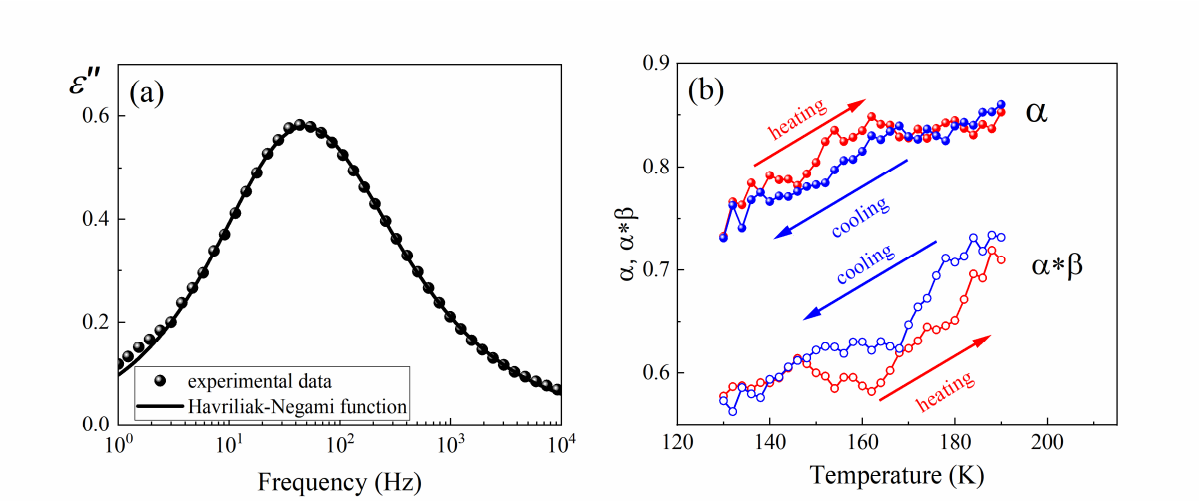

Fig.S7. *Frequency dependence of dielectric losses at 130K fitted with a single Havriliak Negami (HN) function (a). Temperature dependence of the HN power-law exponents characteristic for the relaxation response for cooling and heating cycles (b).*

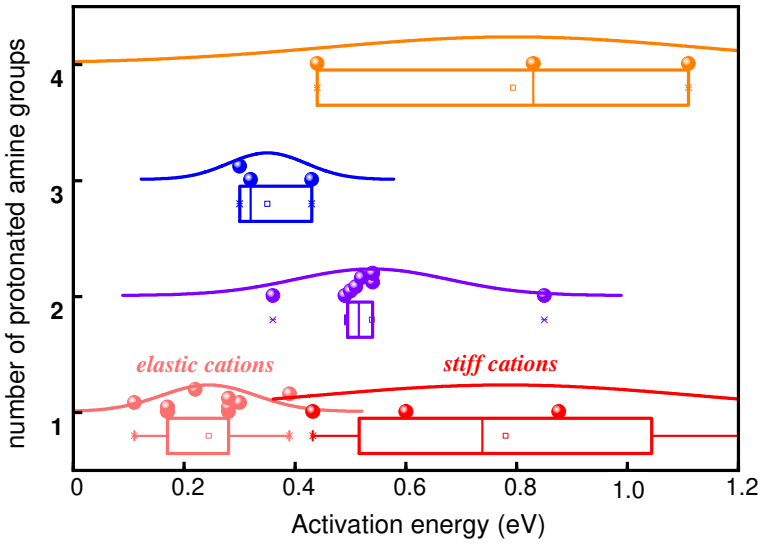

Fig.S8. *Energy barriers for the motion of cage cations in hybrid formates.*

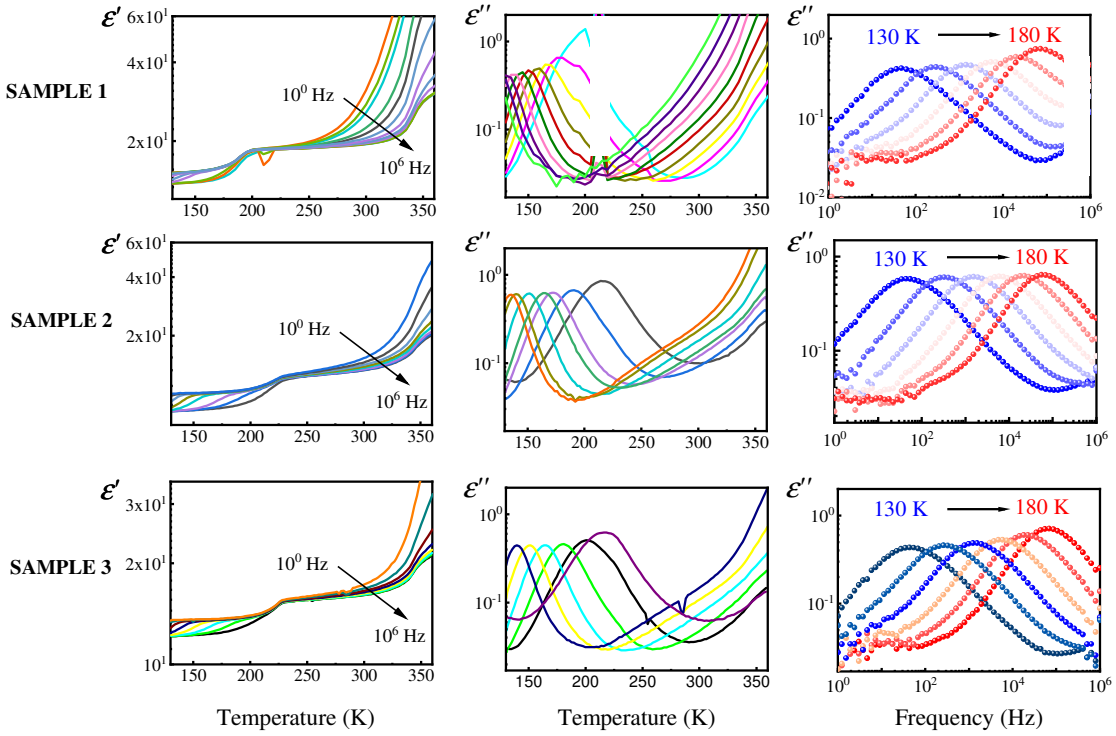

Fig.S9. Comparison of selected $\varepsilon'(T)$, $\varepsilon''(T)$ and $\varepsilon''(f)$ dependences between three pelletized samples of **dptaMn.**

6. Supplementary tables

Table S1. Experimental details

For all structures: $C_{15}H_{29}Mn_3N_3O_{18}$, M_r = 704.23. Experiments were carried out with Mo *K*a radiation using a Xcalibur, Atlas. Absorption was corrected for by multi-scan methods, *CrysAlis PRO* 1.171.38.43 (Rigaku Oxford Diffraction, 2015) Empirical absorption correction using spherical harmonics, implemented in SCALE3 ABSPACK scaling algorithm.. H-atom parameters were constrained.

	Phase I	Phase II	Phase II
Crystal data			
Crystal system, space group	Trigonal, *R*-3*c*:*H*	Monoclinic, *I*2/*a*	Monoclinic, *I*2/*a*
Temperature (K)	360	120	300 K
a, *b*, *c* (Å)	8.5557 (5), 8.5557 (5), 63.715 (4)	28.4792 (15), 8.6388 (4), 32.292 (3)	28.6514 (15), 8.6359 (4), 32.401 (3)
α, β, γ (°)	90, 90, 120	90, 90.303 (6), 90	90, 90.400 (6), 90
V (Å^3)	4039.1 (5)	7944.5 (9)	8016.7(9)
Z	6	12	12
μ (mm^{-1})	1.47	1.50	1.48
Crystal size (mm)	0.21 × 0.08 × 0.05	0.21 × 0.08 × 0.05	0.21 × 0.08 × 0.05
Data collection			
T_{min}, T_{max}	0.939, 1.000	0.873, 1.000	0.896, 1.000
No. of measured, independent and observed [$I > 2\sigma(I)$] reflections	8588, 1182, 748	27213, 9482, 5395	27797, 9769, 4634
R_{int}	0.035	0.053	0.042
$(\sin\theta/\lambda)_{max}$ (Å^{-1})	0.690	0.690	0.690
Refinement			
$R[F^2 > 2\sigma(F^2)]$, $wR(F^2)$, *S*	0.037, 0.103, 1.04	0.064, 0.129, 1.17	0.056, 0.094, 1.01
No. of reflections	1182	9482	9769
No. of parameters	63	541	541
No. of restraints	0	8	2
$\Delta\rangle_{max}$, $\Delta\rangle_{min}$ (e Å^{-3})	0.38, -0.54	0.75, -0.57	0.778, -0.432

Computer programs: *CrysAlis PRO* 1.171.38.43 (Rigaku OD, 2015), *SHELXT* 2018/2 (Sheldrick, 2018), *SHELXT* 2014/5 (Sheldrick, 2014), *SHELXL2018*/3 (Sheldrick, 2018).

Table S2. Selected geometric parameters (Å, º)

(360)			
Mn1—O2^{i}	2.1673 (17)	Mn2—O1	2.1782 (18)
Mn1—O2^{ii}	2.1673 (18)	Mn2—O1^{vi}	2.1783 (18)
Mn1—O2^{iii}	2.1672 (17)	Mn2—O1^{vii}	2.1783 (18)
Mn1—O2^{iv}	2.1672 (17)	Mn2—O3	2.1817 (18)
Mn1—O2	2.1671 (17)	Mn2—O3^{vi}	2.1818 (18)
Mn1—O2^{v}	2.1672 (18)	Mn2—O3^{vii}	2.1819 (18)
(120K)			
Mn1—O5	2.108 (3)	Mn3—O17	2.169 (3)
Mn1—O5^{viii}	2.108 (3)	Mn3—O19	2.173 (3)
Mn1—O3	2.193 (3)	Mn3—O25^{x}	2.194 (3)
Mn1—O3^{viii}	2.193 (3)	Mn4—O22	2.132 (3)
Mn1—O2^{viii}	2.200 (3)	Mn4—O20	2.172 (3)
Mn1—O2	2.200 (3)	Mn4—O26	2.196 (3)
Mn2—O6	2.143 (3)	Mn4—O27^{xi}	2.196 (3)
Mn2—O10	2.164 (3)	Mn4—O18^{ix}	2.201 (3)
Mn2—O12	2.168 (3)	Mn4—O1^{ix}	2.211 (3)
Mn2—O8	2.175 (3)	Mn5—O23	2.132 (3)
Mn2—O11	2.193 (3)	Mn5—O14^{xii}	2.175 (3)
Mn2—O4^{ix}	2.222 (3)	Mn5—O7^{xiii}	2.185 (3)
Mn3—O15	2.151 (3)	Mn5—O24	2.185 (3)
Mn3—O13	2.157 (3)	Mn5—O16^{xiv}	2.195 (3)
Mn3—O21	2.167 (3)	Mn5—O9^{xv}	2.210 (3)

Symmetry code(s): (i) -*x*+4/3, -*y*+2/3, -*z*+2/3; (ii) *x*-*y*+1/3, *x*-1/3, -*z*+2/3; (iii) *y*+1/3, -*x*+*y*+2/3, -*z*+2/3; (iv) -*y*+1, *x*-*y*, *z*; (v) -*x*+*y*+1, -*x*+1, *z*; (vi) -*y*, *x*-*y*, *z*; (vii) -*x*+*y*, -*x*, *z*; (viii) -*x*+1, -*y*+2, -*z*+1; (ix) *x*, *y*-1, *z*; (x) *x*-1/2, -*y*, *z*; (xi) -*x*+1, *y*+1/2, -*z*+3/2; (xii) *x*+1/2, -*y*+1, *z*; (xiii) -*x*+1, -*y*+1, -*z*+1; (xiv) -*x*+1, *y*-1/2, -*z*+3/2; (xv) -*x*+1, -*y*, -*z*+1.

Table S3. Selected hydrogen-bond parameters

D—H···*A*	*D*—H (Å)	H···*A* (Å)	*D*···*A* (Å)	*D*—H···*A* (°)
(120K)				
N2A—H2AA···O3^{i}	0.89	2.15	2.961 (5)	151.4
N2A—H2AA···O4^{i}	0.89	2.57	3.276 (4)	136.5
N2A—H2AB···O25	0.89	2.01	2.862 (4)	160.6
N2A—H2AC···O1^{i}	0.89	2.46	3.195 (4)	140.1
N2A—H2AC···O20^{ii}	0.89	2.45	3.054 (4)	125.1
N1B—H1BA···O13^{iii}	0.89	2.22	2.957 (5)	140.5
N1B—H1BA···O21^{iii}	0.89	2.51	3.223 (5)	137.6
N1B—H1BB···O4^{iv}	0.89	2.24	3.074 (4)	155.3
N1B—H1BC···O2^{iii}	0.89	2.02	2.904 (4)	170.0
N2B—H2BA···O9^{v}	0.89	2.18	3.011 (4)	154.9
N2B—H2BA···O10^{v}	0.89	2.58	3.175 (5)	125.3
N2B—H2BB···O26^{vi}	0.89	2.34	3.142 (4)	150.8
N2B—H2BB···O27^{vi}	0.89	2.40	3.225 (5)	153.4
N3B—H3BA···O18^{vii}	0.89	2.25	3.078 (6)	154.6
N3B—H3BB···O17	0.89	1.96	2.842 (5)	169.4
N3B—H3BC···O16^{viii}	0.89	2.50	3.231 (5)	140.1

Symmetry code(s): (i) x+1/2, -y+1, z; (ii) x+1/2, -y, z; (iii) -x+1, y-1/2, -z+3/2; (iv) -x+1, y-3/2, -z+3/2; (v) x, -y+1/2, z+1/2; (vi) -x+1, y+1/2, -z+3/2; (vii) x, y-1, z; (viii) -x+1/2, -y+1/2, -z+3/2.